DYNAMIC FRACTURE IN CFRP PANELS UNDER COMPRESSIVE LOADING

J. Ankersen[1*], E.S. Greenhalgh[1], S.A. Tsampas[1], P.T. Curtis[2]

[1] *Department of Aeronautics, Imperial College London, UK*
[2] *Physical Sciences Department, DSTL, Wiltshire, UK*
**j.ankersen@imperial.ac.uk*

Keywords: Crack propagation speed, compressive fracture, composites, finite element analysis.

Abstract
Little is known about compression crack velocities, and methods to arrest them. Here a sandwich panel was used for characterisation of rapid crack propagation under compressive loading by means of high speed video in conjunction with Digital Image Correlation (DIC). A finite element modelling approach was developed and compared with the test data. This investigation included plain skin panels and panels with thickened regions which showed evidence of crack retardation.

1 Introduction

An underlying aim of the CRASHCOMPS program is to develop crack arresting features in compression loaded CFRP (Carbon Fibre Reinforced Polymer) panels. Considerable work has been published in the literature concerning the tension and shear regime of quasi-static and dynamic crack arrest including understanding RCP (Rapid Crack Propagation). Impact driven dynamic fracture has been widely studied with Kalthoff style specimens and single-edge notch specimens subjected to short-beam three point bending during impact, with a recent study highlighted in [1]. A wedge driven pre-loaded strip test has also been used for RCP work on UD composites but only with the crack growing along fibres i.e. in a ply-splitting mode [2].

Crack arrest in laminated composites has also been addressed in tension where buffer strips are a recognised means of enhancing damage tolerance [3]. Damage tolerance of stiffened composite compression panels has been investigated at an experimental level [4]. Panels were assessed by inducing impact damage to pre-loaded panels and rating their residual strength, provided the impact had not already caused catastrophic failure. Detailed analysis of crack propagation leading to collapse was, however, not performed. Compressive fracture has received very limited attention in terms of RCP and crack arrest. Within the aerospace industry, compression failure would of course often be associated with buckling. Yet there is a need for an improved understanding of in-plane compression failure to enable design of damage tolerant rather than 'just' fail-safe structures. To this end it was desirable to underpin crack arrest studies using a flat panel where compressive fracture could be generated in a uniform strain field.

This paper presents measurements of RCP in a flat panel under compressive load as well as observations made during development of a FE (Finite Element) model of the problem. The main purpose of the FE modelling capability is to enable development of damage tolerant designs with a focus on survivability of unstable crack growth following relatively severe impact events.

2 Rapid crack propagation

2.1 Test specimen design

For this study, a sandwich design was chosen to avoid the need for anti-buckling guides thus providing a clear view of a relatively large panel surface suitable for crack tip tracking via high speed video. This free surface also enabled the addition of geometric features for the study of crack arrest in compression. The front skin was notched (R=10mm) at one side edge to generate fracture, leaving the back skin of the sandwich panel intact, Fig.1. Skins were 2mm thick with an eight ply quasi-isotropic layup $[45/-45/0/90]_S$ of double thickness (0.25mm nom) HTS/MTM44-1 uni-directional pre-preg material. A 40mm thick aluminium honeycomb core was bonded between the skins with Redux 312 film adhesive and the final sandwich gauge section between end-blocks was 200x200mm. Test samples were loaded to failure in a 250t compression test rig at 0.2mm/min. Some panels incorporated a thickened region in the form of a 2mm thick strip co-cured with the front skin and extending the full height of the panel. The strip had 1:10 tapered edges to prevent debonding and a total width of 60mm thus providing a 20mm wide full thickness section. The outline has been indicated in Fig.3. Other strip configurations are currently under investigation.

2.2 Measurement

Digital high speed footage was used to track the crack tip during propagation. Initial testing made use of a Phantom Miro4 from the EPSRC equipment loan pool. This was capable of 41000fps at a 128x64 resolution which was just adequate for crack tip tracking. A more powerful Vic 3D HS 5400 DIC (Digital Image Correlation) system, also from the EPSRC loan pool, was used in subsequent tests. Here full field surface strain measurement was achieved at 20000fps with a 512x256 resolution. This resolution was the minimum required for acceptable strain calculation across the 200mm wide test area. A high contrast speckle pattern was applied to the specimen prior to testing, Fig.1.

Figure 1. Notched sandwich specimen with thickened region after loading to failure.

Two strain gauges were mounted on the front skin (Fig.1.) and two on the back skin to enable verification of loading uniformity of the sandwich panel. Force readings were recorded from load cells on the test frame and applied displacement was measured by a LVDT (Linear Variable Displacement Transducer) positioned between the loading platens.

2.3 Simulation

Several researchers have attempted to model crack growth, however, these again concern tensile fracture and have mostly used a cohesive zone approach [5,6]. Cohesive elements are suitable for modelling tensile (mode I) and shear (mode II) in-plane fracture but are strictly aimed at delamination modelling. Compressive fracture is, however, not discrete and features a crushing zone which at a meso modelling scale must cover the complex sequence of actual microscale events. For quasi-isotropic laminates this typically includes delamination, in-plane and transverse shear failure and micro-buckling leading to kink band formation and final collapse. The exact sequence of events is still an active research topic [7,8].

Here an energy based smeared approach was used which is more suitable for medium scale in-plane failure modelling and is mesh objective provided the element size remains below:

$$l_x = \frac{2EG_c}{\sigma_c^2} \tag{1}$$

where E is Young's modulus, G_C is the in-plane strain energy release rate and σ_C is the strength, all for the material at ply-level [9].

Property	Unit	Value
Longitudinal modulus	E_{11} [GPa]	123.2
Transverse modulus	E_{22} [GPa]	8.8
Poison's ratio	ν_{12}	0.3
In-plane shear modulus	G_{12} [GPa]	4.2
Fibre tensile strength	X_T [MPa]	2100
Matrix tensile strength	Y_T [MPa]	66
In-plane shear strength	S_C [MPa]	105
Fibre compr strength	X_C [MPa]	950
Matrix compr strength	Y_C [MPa]	200
Fibre tensile toughness	G_{1CT} [KJ/m^2]	90
Matrix tensile toughness	G_{2CT} [KJ/m^2]	0.8
Fibre compr toughness	G_{1CC} [KJ/m^2]	100
Matrix compr toughness	G_{2CC} [KJ/m^2]	10
Delamination		
Mode I toughness	G_{IC} [J/m^2]	300
Mode II toughness	G_{IIC} [J/m^2]	800
Mode I init strength	S_{IC} [Mpa]	66
Mode II init strength	S_{IIC} [Mpa]	105

Table 1. Ply data as used for HTS/MTM44-1.

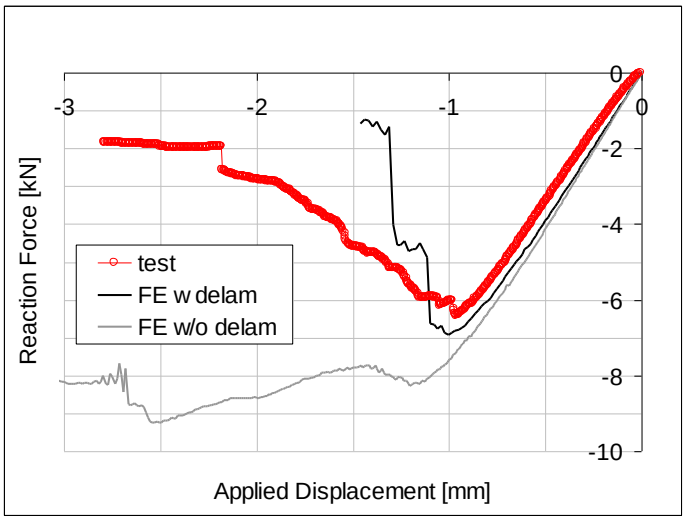

Figure 2. Predicted response with and without delamination versus test response of CC specimen.

Models were run in Abaqus Explicit v6.10 from Simulia. A dynamic explicit approach was taken mainly due to RCP being a truly dynamic event but also to better cope with the severe material level non-linearities. Ply-level mechanical material properties are given in Table 1. Most of these were based on supplier datasheets while the in-plane G_C values were taken from [10]. A plane stress energy based constitutive damage model originating from [9] and enhanced in collaboration with Airbus was used as well as the generic Hashin based damage model. The main enhancements relevant here are the inclusion of Mohr-Coulomb based failure in the matrix dominated compressive σ_{22}-τ_{12} domain [11] and the definition of a debris strength such that some compressive load is still carried after failure.

The compressive fibre strength was still one of the most dominant input parameters in the FE material model. Since micromechanical effects were not explicitly taken into account here, an effective strength value was found by matching FEA data and test data from a CC (Compact Compression) test of the same laminate as used in the sandwich panel, Fig.2. The effect of modelling delamination was also seen as being important, particularly during the propagation stage. Damage actually initiated in the CC specimen earlier than the force-displacement response would suggest in isolation, hence representation of delamination also affected the peak load significantly.

Conventional shell elements were used for some parametric RCP studies including only the notched front skin and ignoring delamination. In more detailed models, delamination was included by meshing the laminate with a continuum shell element (SC8R) per ply and inserting cohesive elements (COH3D8) at all ply interfaces. In either case, uniform end displacement was applied to the gauge section i.e. end blocks were ignored in the model. Computing cost increased by more than an order of magnitude by adding the cohesive elements. Whilst delamination did affect the predicted crack speed, it did not affect the propagation load as was the case in the CC test, probably due to a uniform stress field prior to fracture followed by the highly unstable RCP in the sandwich configuration. Mesh objectivity should be ensured with a mesh size of 3mm according to Eq.1. This was verified by halving the mesh size to 1.5mm which had no effect on the predicted initiation or propagation load or crack speed.

3 Results and comparison

Rapid Crack Propagation under compressive loading was successfully measured with the high speed camera. The crack tip was fairly easy to identify on the images due to the arrow-like surface fracture pattern seen when surface plies consist of angle plies [12]. Sequential images at 41000fps provided a constant crack speed of 1020m/s for the sandwich panel considered here. This is well below the lowest possible shear wave speed C_S=1770m/s based on $C_S = \sqrt{G/\rho}$ for neat resin. The homogenised value is even higher for the actual QI laminate i.e. the crack propagation was sub-sonic. At this temporal resolution, an instantaneous transition from quasi-static to constant rate crack propagation was apparent. This was verified with 75000fps footage from a subsequent test. While not fully understood, this observation has also been made for tensile RCP [5]. As mentioned in Section 2.1, some panels incorporated a thickened region in form of a 2mm thick strip with tapered edges. This caused crack retardation, but not arrest, as illustrated in Fig.3 (taken at 20000fps). The diagonal line indicates a constant crack velocity of 1020m/s as observed at higher frame rates.

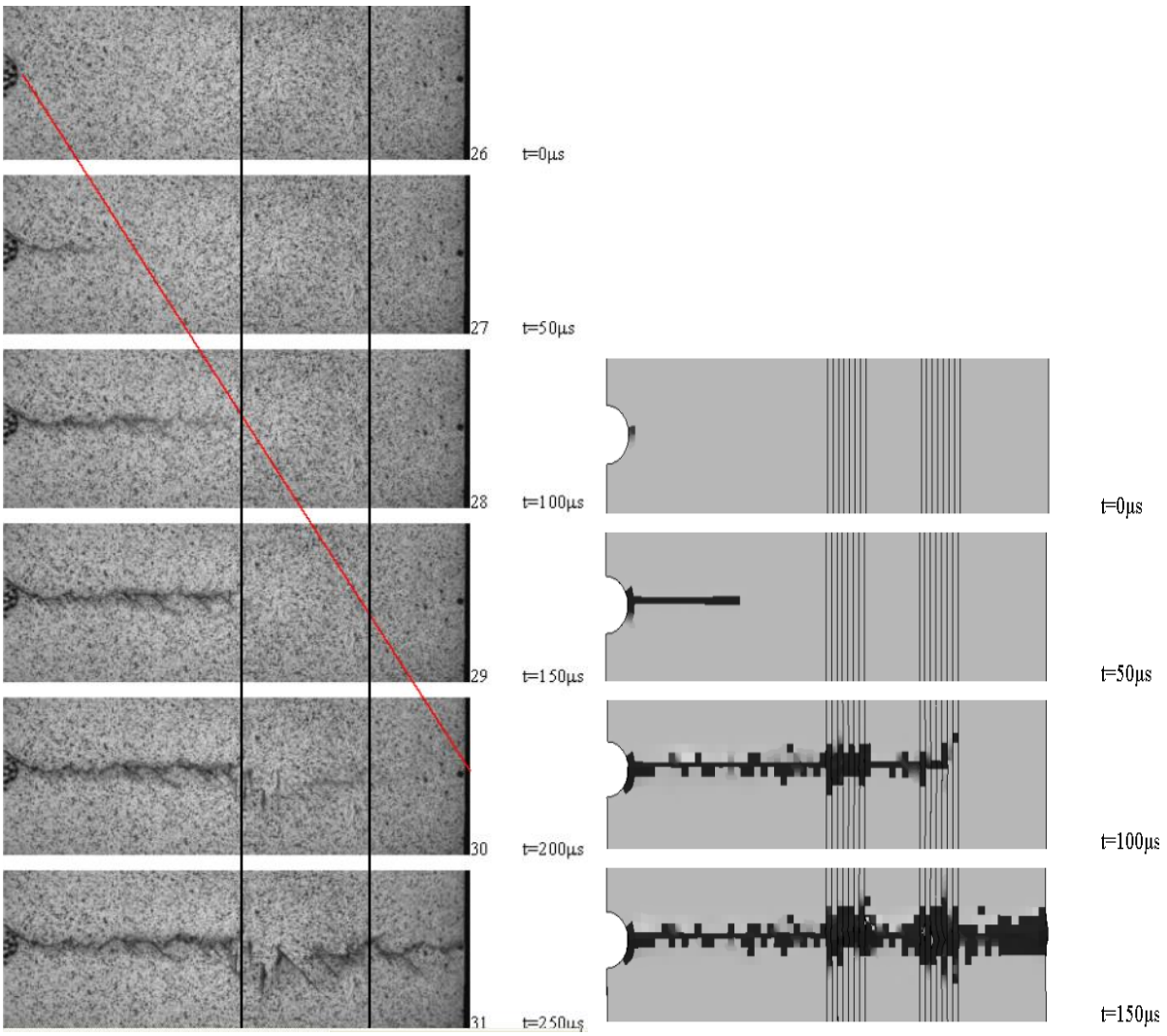

Figure 3. Crack propagation in panel with thickened region (indicated by vertical lines). Measured, diagonal line indicates a constant crack velocity of 1020m/s (left). Predicted propagation (right).

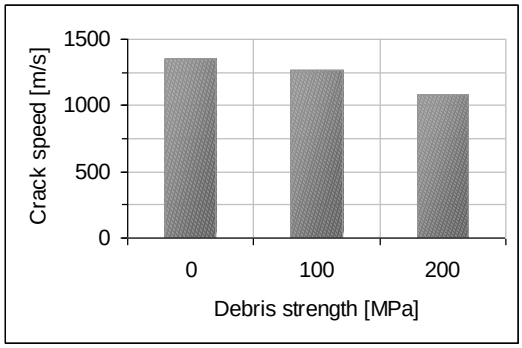

Figure 4. Predicted crack speed versus debris strength.

The FE based crack speed prediction was dependent on several modelling parameters. Inherently, basic material properties such as stiffness and strength affect the crack speed. These were not subjected to sensitivity analysis since the values used were already confirmed by the CC data as well as the force-displacement data from the sandwich test. While the stress based damage initiation criteria did not affect propagation load, the damage growth interaction did. The generic Abaqus Hashin implementation predicted a crack speed of 1900m/s and set the in-plane shear damage to the maximum of any of the direct damage components. This was believed to cause 'fast' degradation and may be the main reason for the high predicted crack speed. The user defined damage model predicted 1360m/s with all parameters set identically but this model does not use any damage growth interaction. The effect of debris strength is shown in Fig.4 where a debris strength of 200MPa reduced the predicted crack speed to 1080m/s. This parameter is difficult to measure on a real specimen since it is highly dependent on the degree of local constraint. Some effect was anticipated since maintaining non-zero stress behind the crack tip will intuitively reduce the strain energy present immediately ahead of the crack tip. The crack speeds stated here are from models where delamination was ignored. Inclusion of delamination lowered the predicted crack speed by approximately 120m/s but increased the analysis time significantly (over an order of magnitude).

A constant crack speed close to the 1020m/s measured in tests was predicted with a flat panel FE model with delamination considered and a debris strength of 100MPa. A FE model of the panel with a thickened region did, however, not predict the crack speed retardation seen in the test, Fig.5. Possible reasons for this are being investigated. The final predicted damage was in

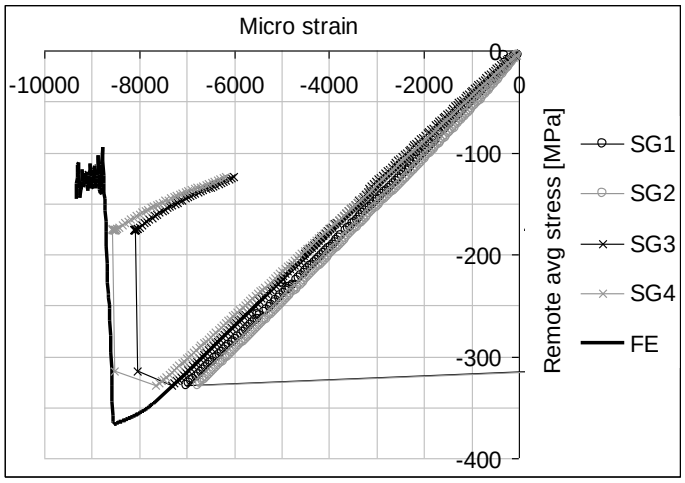

Figure 5. Remote average stress versus strain.

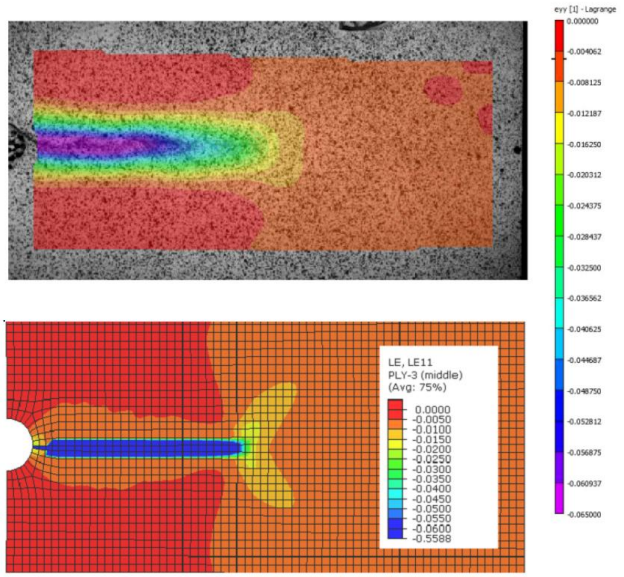

Figure 6. Direct strain in vertical loading direction during RCP. HS DIC (top). FE prediction (bottom).

agreement with that seen in the test specimens (compare Fig.3, left and Fig.3, right). Remote average stress versus strain in the loading direction is shown in Fig.5. for a representative test. The four strain gauges exhibited limited variation, indicating uniform loading. The two gauges on the notched skin (SG1 and SG2) jumped to zero strain at fracture while the gauges on the intact back skin exhibited a new equilibrium. The propagation load (stress) did vary between 226MPa and 370MPa in the nine five tests carried out so far. The FE result is close to the upper value and the predicted panel stiffness matched that of the test panels.

DIC frame rate was limited by resolution requirements but some useful data were obtained. A snapshot of the direct strain distribution during RCP in a flat panel is shown in Fig.6 and compares well with the FE generated strain distribution at the same reference time t=100μs. Detailed information near the crack tip was, however, obscured by the surface plies splaying out under compressive failure. This was a drawback to the DIC method which was not encountered in tension where Lee et al [1] were able to extract data sufficiently accurate for stress intensity calculations. Focusing on higher frame rates with resolutions below DIC requirements was deemed more valuable for the compressive load case.

4 Conclusions

Rapid crack propagation in a typical aerospace grade laminate under compressive loading was measured. The measured and predicted crack speed of 1020m/s was below the shear wave speed of the QI laminate. A detailed FE model was necessary to model RCP in a composite laminate. Good predictions were achieved in terms of propagation load and speed for a flat panel. Crack speed retardation was, however, not predicted sufficiently accurately in a panel with a thickened region. The model will be developed further and used to study crack deflecting and crack arresting features.

Acknowledgements

The work presented here was carried out under the CRASHCOMPS program for which the support by EPSRC and dstl is gratefully acknowledged.

References

[1] D. Lee, H. Tippur, M. Kirulige and P. Bogert. Experimental Study of Dynamic Crack Growth in Unidirectional Graphite/Epoxy Composites using Digital Image Correlation Method and High-speed Photography. *Journal of Composite Materials,* **43(**19), pp. 2081–2108 (2009).

[2] P.N. Kousiounelos and J.H. Williams Jr. Dynamic fracture of unidirectional graphite fiber composite strips. *International Journal of Fracture*, **20**, pp. 47-63 (1982).

[3] C.S. Chu. Crack arrest and residual strength of composite panels with softening strips. *Journal of Aerospace Engineering,* **4**(1), pp. 78-90 (1991).

[4] M.D. Rhodes and J.G. Williams. Concepts for improving the damage tolerance of composite compression panels, NASA TM 85748, February 1984.

[5] F. Costanzo, and J.R. Walton. A study of dynamic crack growth in elastic materials using a cohesive zone model. *International Journal of Engineering Science*, **35**(12/13), pp. 1085-1114 (1997).

[6] Z.J. Zhang and G.H. Paulino. Cohesive zone modeling of dynamic failure in homogeneous and functionally graded materials. *International Journal of Plasticity*, **43**(19), pp. 1195–1254 (2005).

[7] R. Gutkin, S.T. Pinho, P. Robinson and P.T. Curtis. On the transition from shear-driven fibre compressive failure to fibre kinking in notched CFRP laminates under longitudinal compression. *Composites Science and Technology*, **70**(8), pp. 1223-1231 (2010).

[8] S.A. Tsampas, E.S. Greenhalgh, J. Ankersen and P.T. Curtis. On compressive failure of multidirectional fibre-reinforced composites: A fractographic study. *Composites Part A*, **43**(3), pp. 454-468 (2012).

[9] L. Iannucci, and M.L. Willows. An energy based damage mechanics approach to modelling impact onto woven composite materials - Part I: Numerical models. *Composites Part A*, 37, pp. 2041–2056 (2006).

[10] S.T. Pinho, P. Robinson and L. Iannucci. Fracture toughness of the tensile and compressive fibre failure modes in laminated composites. *Composites Science and Technology*, **66**, pp. 2069–2079 (2006).

[11] C.G. Davila, P.P. Camanho and C.A. Rose. Failure Criteria for FRP Laminates. *Journal of Composite Materials*, **39**, pp. 323-345 (2005).

[12] E.S. Greenhalgh and P.C. Cox. A method to determine propagation direction of compressive fracture in carbon-fibre composites. *Composite Structures*, **21**, pp. 1-7 (1992).